The influence of the cloud shell on bulk tracer measurements of LES cloud entrainment

Jordan T Dawe * and Philip H Austin

Department of Earth and Ocean Sciences, University of British Columbia, Vancouver, BC, Canada.

* *Corresponding author address:* Jordan T Dawe, Department of Earth and Ocean Sciences, University of British Columbia, 6339 Stores Road, Vancouver, BC, V6T 1Z4, Canada.

E-mail: jdawe@eos.ubc.ca

ABSTRACT

Direct measurements of rates of entrainment into and detrainment from cloud cores obtained from LES model cloud fields produce values twice as large as those produced from bulk conserved tracer budget calculations. This difference can be explained by three effects: the presence of a shell of moist air around the cloud cores and drier air at the edge of the cloud core, correlations between entrainment rates and tracer values, and errors in the calculation of the bulk tracer budget. Correlations between the vertical momentum and the entrainment rate create strong vertical momentum fluxes into the cloud core, making the assumption that clouds entrain fluid with zero vertical momentum incorrect. Variability in the properties of the moist cloud shell has strong impacts on entrainment values inferred from bulk tracer calculations. These results indicate the dynamics of the cloud shell should be included in parametrization of cumulus clouds used in general circulation models.

1. Introduction

The rate at which air is entrained into and detrained from cumulus clouds affects cloud properties, cloud top height, and vertical transports of heat and moisture. Proper simulation of these sub-grid scale effects in General Circulation Models (GCM) depends on the accurate parametrization of entrainment of environmental tracer properties into the clouds and detrainment of cloud properties into the environment (Bechtold et al. 2008; de Rooy and Siebesma 2010).

Entrainment and detrainment rates impact GCM parametrization in several ways. First, profiles of cloud vertical mass flux are usually calculated from parametrized entrainment

values using the continuity equation for a simple entraining plume:

$$\rho \frac{\partial a}{\partial t} + \frac{\partial M_{core}}{\partial z} = E - D. \tag{1}$$

Here ρ is the density of the air in kg m^{-3}; a is the fractional cloud core area (where cloud core is defined as regions having condensed liquid water, positive buoyancy, and upward vertical velocity); M_{core} is vertical cloud core mass flux (kg m^{-2} s^{-1}) and E and D are mass entrainment and detrainment rates (kg m^{-3} s^{-1}).

The point where the mass flux profile goes to zero then defines the location of cloud top. This mass flux profile is combined with the entrainment rate of environmental air into the cloud to generate vertical profiles of cloud moisture and temperature, and these profiles are then used to calculate the moistening of the environment by detrainment of cloud fluid (Tiedtke 1989; Kain and Fritsch 1990). Precipitation rates are also generated from the mass flux and tracer profiles produced from the entrainment and detrainment profiles. The wide range of effects that the entrainment and detrainment have make entrainment rate one of the strongest controls on the climate sensitivity of GCMs (Stainforth et al. 2005; Rougier et al. 2009).

Large Eddy Simulation (LES) is the primary tool used to study cloud entrainment and detrainment rates. LES mass entrainment and detrainment rates are typically calculated using budgets of bulk conserved tracer variables to infer the amount of fluid exchange between the clouds and the surrounding air. Siebesma and Cuijpers (1995) derive the following equations for entrainment and detrainment of mass from a cloud core plume:

$$E_{\phi S}(\phi_{core} - \phi_{env}) = -M_{core}\frac{\partial \phi_{core}}{\partial z} - \frac{\partial \rho a \overline{w'\phi'}^{core}}{\partial z} - \rho a \frac{\partial \phi_{core}}{\partial t} + a\rho \left(\frac{\partial \bar{\phi}}{\partial t}\right)_{forcing} \tag{2a}$$

and

$$D_{\phi S}(\phi_{core} - \phi_{env}) = -M_{core}\frac{\partial \phi_{env}}{\partial z} + \frac{\partial \rho(1-a)\overline{w'\phi'}^{env}}{\partial z} + \rho(1-a)\frac{\partial \phi_{env}}{\partial t} - \rho(1-a)\left(\frac{\partial \bar{\phi}}{\partial t}\right)_{forcing} \tag{2b}$$

Where ϕ (with units denoted by $[\phi]$) represents any conserved bulk tracer, such as the total specific humidity q_t (kg water kg^{-1} moist air) or the liquid-water moist static energy h (J kg^{-1}); w is vertical velocity (m s^{-1}); *env* and *core* sub-and super-scripts denote horizontally averaged values conditionally sampled in the cloud environment and core; $forcing$ refers to tracer sources and sinks, such as radiation or subsidence, not included in the other terms; primed values represent anomalies relative to the horizontal mean; overbars represent horizontal averaging; and $E_{\phi S}(z)$ and $D_{\phi S}(z)$ are the total mass entrainment into and detrainment from the cloud core inferred from the bulk tracer budget, in kg s^{-1} m^{-3}. We use the S subscript to differentiate E and D calculated via the Siebesma bulk tracer budget method from other measures of mass exchanges, and we shall refer to values calculated by this method as "Siebesma tracer budget" entrainment and detrainment. For convenience, the various tracer and entrainment/detrainment rate subscripts used below are summarized in the Appendix.

Alternatively, entrainment and detrainment of mass can be calculated directly from the LES velocity and tracer fields. Romps (2010) recently presented a technique to measure local (grid scale) mass entrainment $e(x, y, z)$ and detrainment $d(x, y, z)$. Summing these point measurements horizontally gives $E_d(z)$ and $D_d(z)$, the total mass entrained into and detrained from the cloud core field in kg s^{-1} m^{-3}, where the d subscript indicates these quantities were calculated directly from the model velocity and tracer fields. His equation

(2) is:

$$e - d = \frac{\partial}{\partial t}(\mathcal{A}\rho) + \nabla \cdot (\rho \mathbf{u} \mathcal{A}) \tag{3}$$

Here $\mathcal{A}$ is the "activity" of the fluid, where $\mathcal{A}$ is one at cloud core points and zero otherwise, and $\mathbf{u}$ is the velocity of the air in m s^{-1}. The values of $e - d$ are averaged over the time that a grid cell experiences mass fluxes between an active and an inactive point, then positive $e - d$ values are considered to be purely e, and negative values, d. As noted above, we shall refer to entrainment and detrainment values calculated by this method as "direct" E and D and denote them with the subscript d.

Romps found that direct calculation of the entrainment and detrainment mass fluxes produced values roughly twice as large as the Siebesma tracer budget calculations. Romps attributed this difference to the Siebesma tracer budget calculation assumption that fluid exchanged between clouds and environment has the mean properties of the cloud or environment, respectively. Recent studies of the dense, descending shell of moist air that forms around trade-wind cumulus clouds (Heus and Jonker 2008; Wang and Geerts 2010) suggest that the cloud shell properties are quite different than the core or environment properties, bolstering Romps' hypothesis. Since fluid exchanges between clouds and environment must pass through this shell, it is likely that it plays an important role in entrainment and detrainment dynamics.

Below we examine the sources of the discrepancy in entrainment and detrainment values calculated via bulk tracer budgets and directly from model fluxes. We show that the discrepancy is explained by three effects: the presence of the shell of moist air around the cloud cores and drier air at the edge of the cloud core, correlations between local entrainment rates

and tracer values which enhance tracer fluxes between the clouds and the environment, and errors in the calculation of the bulk tracer budget. We derive a relation to transform the "direct" entrainment flux values into "Siebesma tracer budget" values suitable for use in one-dimensional simple entraining plume cloud parametrizations, and then use these transformed fluxes to evaluate the impact of the shell on bulk tracer entrainment and detrainment rates of specific humidity and vertical velocity. Finally, we examine the dynamics that drives the strong correlations we find between entrainment rate, specific humidity, and vertical velocity.

2. Model description

All LES calculations in this paper were made using the System for Atmospheric Modeling (SAM; Khairoutdinov and Randall 2003). Two model runs were performed, configured as standard Global Energy and Water Cycle Experiment (GEWEX) Cloud System Studies (GCSS; Randall et al. 2003) experiments: a Barbados Oceanographic and Meteorological Experiment (BOMEX; Siebesma et al. 2003) run, and an Atmospheric Radiation Measurement Study (ARM; Brown et al. 2002) run. The BOMEX run was performed on a 6.4 km x 6.4 km horizontal x 3.2 km vertical domain with 25 meter grid size in all directions for 6 hours, and the first three hours of simulation were discarded. The ARM run was performed on a 7.68 km x 7.68 km x 4.5 km domain with 30 meter grid size. Precipitation was disabled in both runs.

We have implemented the entrainment calculation scheme of Romps (2010) in SAM, allowing us to calculate the mass of air entrained into and detrained from cloud core directly from model ρ, $\mathbf{u}$, and $\mathcal{A}$. Romps (2010, eq. 4) also presents a method for calculating local

entrainment and detrainment rates for any model bulk variable in the same framework as (3), but neglects forcing and diffusion terms. These terms are significant for quantities like vertical momentum, so we modify Romps' equation to include their effects:

$$e\phi - d\phi = \frac{\partial}{\partial t}(\phi \mathcal{A} \rho) + \nabla \cdot (\phi \rho \mathbf{u} \mathcal{A}) - \rho \mathcal{A} S_\phi \tag{4}$$

where S_ϕ is any non-advective source or sink term for ϕ, such as precipitation for q_t or radiation for h, in units of $[\phi]$ s^{-1}.

As with equation (3), the local $(e\phi)(x,y,z)$ and $(d\phi)(x,y,z)$ must be horizontally summed to give the total tracer entrained into or detrained out of the cloud ensemble, but since ϕ can be negative, it is possible for entrainment to reduce and for detrainment to increase the quantity of tracer in the cloud core. To accommodate this effect, if the average value of ϕ is positive over the time that a grid cell experiences mass fluxes between an active and an inactive point, then positive $e\phi - d\phi$ values are considered to be purely $e\phi$, and negative values, $d\phi$. However, if the average of ϕ is negative, then positive $e\phi - d\phi$ values are considered to be purely $(d\phi)(x,y,z)$, and negative values, $(e\phi)(x,y,z)$. Horizontal summation of $(e\phi)$ and $(d\phi)$ then gives $(E\phi)_d(z)$ and $(D\phi)_d(z)$, the total entrainment and detrainment of tracer for the cloud ensemble in units of $[\phi]$ kg s^{-1} m^{-3} calculated directly from the model velocity and tracer fields.

3. Relationship Between Direct and Bulk Tracer Budget Entrainment

Romps (2010) established that the direct estimate of mass entrainment and detrainment

yields values roughly twice the size of those calculated via bulk tracer budgets. Furthermore, examination of the ratios of the Siebesma tracer budget mass entrainment and detrainment calculated via a total specific water budget (E_{qS}, D_{qS}) to the directly calculated values (E_d, D_d) over the diurnal cycle of an ARM LES reveals significant changes over the course of the day (Fig. 1). Thus the bulk tracer and direct measurements of E and D are not only significantly different, but have differing dynamics, which may need to be be accounted for in large-scale parametrizations that account for entrainment and detrainment. In this section we examine the sources of disagreement between direct and Siebesma tracer budget estimates of mass entrainment into and detrainment from the cloud core. We first consider the different assumptions about tracer values in the cloud core and environment, then look at correlations between entrainment/detrainment and tracer values and the different numerical approximations made in the two budget calculations.

a. E and D Cloud Shell Correction

Romps attributed the differences between ($E_{\phi S}$, $D_{\phi S}$) and (E_d, D_d) to the assumption made by Siebesma and Cuijpers (1995) that fluid entrained or detrained has the properties of the mean environment or cloud core, respectively. The fact that the mean core and environment properties are not representative of entraining and detraining fluid is shown in Fig. 2a. If we examine the specific humidity of the fluid at the "cloud core edge" (cloud core model grid cells that are nearest-neighbor adjacent to non-core cells), which presumably is the fluid being detrained, we see it is drier than the mean core. Similarly, the fluid just outside the cloud core in the "cloud core shell" (non-core model grid cells that are nearest-

neighbor adjacent to core cells) which is available for entrainment is moister than the mean environment.

Budget equations that explicitly distinguish between the the moist cloud shell and dry cloud edge allow us to transform (E_d, D_d) values into equivalent Siebesma tracer budget values $(E_{\phi S}, D_{\phi S})$ and back again. We start our derivation by modifying equations (5.1) from Siebesma and Cuijpers (1995):

$$\rho\frac{\partial a\phi_{core}}{\partial t} = -\frac{\partial M_{core}\phi_{core}}{\partial z} + E_d\phi_E - D_d\phi_D - \frac{\partial \rho a\overline{w'\phi'}^{core}}{\partial z} + a\rho\left(\frac{\partial\bar{\phi}}{\partial t}\right)_{forcing} \tag{5}$$

$$\rho\frac{\partial (1-a)\phi_{env}}{\partial t} = \frac{\partial M_{core}\phi_{env}}{\partial z} - E_d\phi_E + D_d\phi_D - \frac{\partial \rho(1-a)\overline{w'\phi'}^{env}}{\partial z} + \rho(1-a)\left(\frac{\partial\bar{\phi}}{\partial t}\right)_{forcing}. \tag{6}$$

Here we have replaced ϕ_{env} in the original entrainment term with ϕ_E and ϕ_{core} in the detrainment term with ϕ_D, where ϕ_E and ϕ_D are the tracer values of the air being entrained and detrained, respectively.

Next we substitute equation (1), the continuity equation for a cloud plume, into (5) and (6) and using the chain rule write

$$E_d(\phi_{core}-\phi_E) - D_d(\phi_{core}-\phi_D) = M_{core}\frac{\partial\phi_{core}}{\partial z} + \frac{\partial \rho a\overline{w'\phi'}^{core}}{\partial z} + \rho a\frac{\partial\phi_{core}}{\partial t} - a\rho\left(\frac{\partial\bar{\phi}}{\partial t}\right)_{forcing} \tag{7}$$

$$D_d(\phi_D-\phi_{env}) - E_d(\phi_E-\phi_{env}) = -M_c\frac{\partial\phi_{env}}{\partial z} + \frac{\partial \rho(1-a)\overline{w'\phi'}^{env}}{\partial z} + \rho(1-a)\frac{\partial\phi_{env}}{\partial t} - \rho(1-a)\left(\frac{\partial\bar{\phi}}{\partial t}\right)_{forcing}$$

We then substitute in (2) for the bulk tracer tendency terms and rearrange to get:

$$E_{\phi T} = E_d - \left[E_d\frac{(\phi_E-\phi_{env})}{(\phi_{core}-\phi_{env})} + D_d\frac{(\phi_{core}-\phi_D)}{(\phi_{core}-\phi_{env})}\right] \tag{9a}$$

$$D_{\phi T} = D_d - \left[E_d\frac{(\phi_E-\phi_{env})}{(\phi_{core}-\phi_{env})} + D_d\frac{(\phi_{core}-\phi_D)}{(\phi_{core}-\phi_{env})}\right]. \tag{9b}$$

The bracketed terms represent the bias introduced by assuming that entrained/detrained air has the properties of the mean environment and core. Thus, to convert from (E_d,D_d) to ($E_{\phi T}$, $D_{\phi T}$), both E_d and D_d must be reduced by $E_d A + D_d B$, where $A = (\phi_E - \phi_{env})/(\phi_{core} - \phi_{env})$ and $B = (\phi_{core} - \phi_D)/(\phi_{core} - \phi_{env})$. Here we have added the T subscript to the $E_{\phi T}$ and $D_{\phi T}$ terms to denote that these values are equivalent to Siebesma tracer budget values, but have been calculated by transforming the direct entrainment and detrainment values. We shall refer to these values as "transformed" entrainment and detrainment.

Alternatively, we can solve for E_d and D_d, arriving at

$$E_{dT} = E_{\phi S} + \left[E_{\phi S} \frac{(\phi_E - \phi_{env})}{(\phi_D - \phi_E)} + D_{\phi S} \frac{(\phi_{core} - \phi_D)}{(\phi_D - \phi_E)} \right]. \tag{10a}$$

$$D_{dT} = D_{\phi S} + \left[E_{\phi S} \frac{(\phi_E - \phi_{env})}{(\phi_D - \phi_E)} + D_{\phi S} \frac{(\phi_{core} - \phi_D)}{(\phi_D - \phi_E)} \right]. \tag{10b}$$

In this case, to convert from ($E_{\phi S}$, $D_{\phi S}$) to (E_{dT}, D_{dT}), both $E_{\phi S}$ and $D_{\phi S}$ must be increased by $E_{\phi S} a + D_{\phi S} b$, where $a = (\phi_E - \phi_{env})/(\phi_{core} - \phi_{env})$ and $b = (\phi_{core} - \phi_D)/(\phi_{core} - \phi_{env})$. Note that under both these transformations $E_d - D_d = E_\phi - D_\phi$, preserving mass continuity, and furthermore, $E_d A + D_d B = E_\phi a + D_\phi b$.

We now have relationships allowing us to transform the unbiased E_d and D_d values into biased Siebesma tracer budget $E_{\phi S}$ and $D_{\phi S}$ values, which are better suited for simple entraining plume parametrization of cloud fields. Comparison of E_{qS} and D_{qS} ($E_{\phi S}$ and $D_{\phi S}$ inferred using total specific moisture q_t as the bulk tracer) with E_d and D_d shows the direct entrainment and detrainment magnitudes are significantly larger than the Siebesma tracer budget values (Figure 2b and 2c, grey and dotted lines). Using (9) to calculate E_{qT} and D_{qT} with $q_E = q_{edge}$ and $q_D = q_{shell}$ results in values quite close to the Siebesma tracer budget values above the middle of the cloud layer. The transformation also duplicates the negative

detrainment values near cloud base that are typically produced by bulk tracer calculations.

b. Entrainment/Tracer Correlations

Relative to the Siebesma tracer budget values, the transformed E_{qT} and D_{qT} values are still too large near cloud base. We can partially explain the difference between the transformed mass entrainment/detrainment values and the Siebesma tracer budget values as being the result of correlations between the local entrainment/detrainment rates and the local tracer properties in the shell and edge. Using the mean shell and edge values of tracers to transform the direct entrainment and detrainment assumes that any fluid parcel in the shell or edge is equally likely to be entrained or detrained. In reality, mixing relatively dry air into the cloud core is more likely to cause evaporation, which will drive detrainment, while mixing relatively moist air into the cloud core is more likely to produce a saturated fluid mixture, resulting in entrainment.

If there are correlations between entrainment/detrainment and the local fluid properties, this will result in the effective tracer value entrained into or detrained from the cloud core being different than the mean tracer value in the shell or edge. We can directly calculate the effective tracer value at which entrainment occurs by taking the total tracer entrainment $(E\phi)_d$ calculated via equation (4) and dividing it by the total mass entrainment E_d so that $\phi_{entrain} = (E\phi)_d/E_d$. Similarly, the effective tracer value at which detrainment occurs can be found from $\phi_{detrain} = (D\phi)_d/D_d$. Examination of these values from the BOMEX simulation using q_t for ϕ shows $q_{entrain}$ is moister than q_{shell} (Figure 3a), indicating entrainment occurs preferentially at the moistest parts of the shell. Conversely, there is little difference between

between $q_{detrain}$ and q_{edge}, indicating no significant correlation between detrainment and the moisture present in the cloud core edge.

Using $q_{entrain}$ and $q_{detrain}$ to transform E_d and D_d results in smaller E_{qT} and D_{qT} values than utilizing the mean shell and edge properties (solid black line, Fig. 3b and 3c). E_{qT} calculated using $q_E = q_{entrain}$ and $q_D = q_{detrain}$ is about half the magnitude of the Siebesma tracer budget entrainment value throughout the cloud layer. This new transformation reduces the large entrainment and detrainment values near cloud base, which improves the overall shape of the fluxes. Above mid-cloud, however, there is less correspondence between transformed E_{qT} and D_{qT} values and the Siebesma tracer budget values E_{qS} and D_{qS} when compared to the shell and edge correction of Figure 3.

c. Tracer Budget Errors

The results above highlight the role of the definition of mean cloud and environmental quantities in determining entrainment and detrainment using tracer budgets. An additional source for the discrepancy between the bulk tracer budgets and their direct counterparts is the calculation of source and sink terms. The Siebesma tracer budget calculated using (2) accounts for the vertical advection of tracer properties by taking derivatives of mean vertical tracer profiles, along with averaged vertical Reynolds fluxes. There is no guarantee this estimate of vertical advection will exactly agree with the fully three dimensional MPDATA advection algorithm used by SAM. In fact, the differences in the numerics of these calculations likely insures the results, while similar, will not be exactly the same. Furthermore, the Siebesma calculation neglects tracer diffusion. These effects are likely small, but the exact

amount of error they induce is difficult to evaluate.

Romps (2010) presents an alternative to the Siebesma method of calculating bulk tracer budget entrainment and detrainment values (Romps' equations (11) and (12)) which uses the direct mass and ϕ entrainment/detrainment rates and mean profiles of ϕ_{core} and ϕ_{env} to calculate the vertical advection and time tendency budgets (referred to as VATT below) that are on the right hand side of (2):

$$E_{\phi R}(\phi_{core} - \phi_{env}) = \phi_{core}(E_d - D_d) - ((E\phi)_d - (D\phi)_d) \tag{11a}$$

$$D_{\phi R}(\phi_{core} - \phi_{env}) = \phi_{env}(E_d - D_d) - ((E\phi)_d - (D\phi)_d) \tag{11b}$$

Here the R subscript indicates that E and D have been calculated via the Romps bulk tracer budget method, and we shall refer to values calculated by this method as the "Romps tracer budget" E and D.

To see that the Romps tracer budget equations (11) account for exactly the same source and sink terms as the Siebesma tracer budget equations (2), first multiply (1) by ϕ_{core}:

$$\phi_{core}(E_d - D_d) = \phi_{core}\left(\rho\frac{\partial a}{\partial t} + \frac{\partial M_{core}}{\partial z}\right). \tag{12}$$

If diffusion is neglected, the tracer continuity equation can be used to show that

$$(E\phi)_d - (D\phi)_d = \rho\frac{\partial(a\phi_{core})}{\partial t} + \frac{\partial(M_{core}\phi_{core})}{\partial z} + \frac{\partial\rho a\overline{w'\phi'}^{core}}{\partial z} - a\rho\left(\frac{\partial\bar{\phi}}{\partial t}\right)_{forcing}. \tag{13}$$

Subtracting $(E\phi)_d - (D\phi)_d$ from $\phi_{core}(E_d - D_d)$ then results in the VATT budget terms on the rhs of (2a).

Note that by substituting $(E\phi)_d = E_d\phi_E$ and $(D\phi)_d = D_d\phi_D$ into (11), we can quickly recover the equations to transform direct entrainment/detrainment values into equivalent

tracer budget values (equations (9a) and (9b)). This equivalence between (9) and (11) means the Romps tracer budget formulation agrees exactly with the result of using $q_{entrain}$ and $q_{detrain}$ values to transform the direct entrainment and detrainment into equivalent bulk tracer values.

Comparing the Romps and Siebesma $q_{core}(E_d - D_d)$ values (Fig. 4a) shows that the Romps value for this first VATT term has a significantly smaller magnitude than the Siebesma value given by (2). The Romps $(Eq_t)_d - (Dq_t)_d$ values (Fig. 4b) also have a smaller magnitude when compared to the Siebesma value. The reason for this can be seen by comparing these calculations with a version of the direct entrainment calculation done without any time averaging of the fluxes. The effect of time averaging is to significantly reduce the size of the direct entrainment and detrainment rates E and D. The difference $E - D$, however, is the same with or without time averaging in order to satisfy mass continuity as expressed by (1). Indeed, the unaveraged $\phi_{core}(E_d - D_d)$ value (gray line in Figure 4a) agrees almost exactly with the Siebesma tracer budget value $\phi_{core}(E_{qS} - D_{qS})$ (dotted line). Due to the time averaging of the direct entrainment and detrainment, the direct calculation always has a pool of "activity flux" which has not yet been assigned to either E_d or D_d. This reduces both E_d and D_d by roughly the same proportion, causing $E_d - D_d$ to be smaller than both the unaveraged direct values and the Siebesma $E_{qS} - D_{qS}$ values.

However, despite the large differences between the time averaged $q_{core}(E_d - D_d)$ and $((Eq_t)_d - (Dq_t)_d)$ values and the unaveraged values, the net tracer budget that results from the difference between these terms (Fig. 4c) agrees remarkably well. Conversely, the Siebesma tracer budget that results is much larger than the Romps tracer budget, despite the close agreement between the Siebesma and Romps tracer budget $q_{core}(E_d - D_d)$ and $((Eq_t)_d -$

$(Dq_t)_d$) values. This difference between the tracer budgets calculated by the Siebesma and Romps methods is the source of the remaining differences between the direct and Siebesma entrainment and detrainment calculations.

Evaluating whether the VATT budget calculation done using (2) or (11) is more accurate is difficult. We have mentioned the possible problems in the Siebesma tracer budget calculation related to neglect of tracer diffusion and the simplified method used to calculating vertical advection. The Romps tracer budget, on the other hand, requires taking the difference of $q_{core}(E_d - D_d)$ and $((Eq_t)_d - (Dq_t)_d)$, terms which have nearly the same magnitude. Because the magnitude of these terms is so similar, small relative errors in these terms can result in large relative errors when their difference is taken. Consider, for example, the tiny difference between the unaveraged direct $((Eq_t)_d - (Dq_t)_d)$ and the Siebesma $((Eq_t)_d - (Dq_t)_d)$ calculated via (13) (Fig. 4b). Although the Siebesma tracer budget $((Eq_t)_d - (Dq_t)_d)$ differs only slightly from the unaveraged direct flux value, this results in a relatively large difference between the unaveraged direct tracer budget and Siebesma tracer budgets (Fig. 4c). Both of the calculation methods thus have possible sources of error.

4. E_q, E_h and E_w Differences

Equations (9a) or (9b) imply that the Siebesma tracer budget method will measure different entrainment and detrainment values for fluid properties with differing values of $A = (\phi_E - \phi_{env})/(\phi_{core} - \phi_{env})$ and $B = (\phi_{core} - \phi_D)/(\phi_{core} - \phi_{env})$. With this in mind we compare transformed $E_{\phi T}$ and $D_{\phi T}$ values produced by liquid water moist static energy h and vertical velocity w with those produced using total specific moisture q_t.

Liquid water moist static energy shows a similar relative distribution of core, edge, shell, environment, entrained, and detrained properties when compared to q_t, indicating a tight coupling between these variables in the cloud dynamics. Because these properties are so tightly coupled, the transformed E_{hT} and D_{hT} values are nearly identical to the E_{qT} and D_{qT} (not shown).

Vertical velocity shows very different relative profiles compared to q_t or h (c.f. Fig. 5a and Fig. 3a). There is a much wider spread in the w values, with the shell having nearly zero vertical velocity and the edge being halfway between the core and the environment. $w_{detrain}$ is slightly larger than the value of w in the cloud core edge, while $w_{entrain}$ is much larger than w in the shell, becoming roughly the same value as w_{edge}. Since $w_{entrain}$ and $w_{detrain}$ are both larger than w_{shell} and w_{edge} this implies that rapidly rising air is both preferentially entrained and detrained over slowly rising air. These effective entrainment and detrainment w values produce E_{wT} and D_{wT} (solid black line, Fig. 5c and Fig. 5c) that are quite different than the transformed entrainment and detrainment produced by q_t and h (dotted line, Fig. 5b and 5c); E_{wT} is negative over the whole of the cloud field, and D_{wT} is half the magnitude of D_{qT} over much of the cloud layer.

Finally, we examine the temporal variability of $A = (\phi_E - \phi_{env})/(\phi_{core} - \phi_{env})$ and $B = (\phi_{core} - \phi_D)/(\phi_{core} - \phi_{env})$ from the transformation equations (9a) and (9b) in the ARM model run. These quantities show strong changes over the ARM diurnal cycle (Figure 6). Near cloud base and within the inversion, A is nearly one while B is nearly zero. As the clouds mix into the inversion over the course of the day, the values calculated using q_t evolve until at mid-cloud layer, A has values near 0.6 and B near 0.2. When calculated for w on the other hand, A reaches a value around 0.5 and B goes to 0.6. Performing this

calculation with fixed values of $(\phi_{core} - \phi_{env})$, to remove changes due to movement of the mean environment and core profiles, shows similar results. Changes in the properties of the entraining and detraining fluid clearly are active in determining the magnitude of the rates at which properties entrain and detrain.

5. Causes of e, q, and w Correlations

The source of the correlations between entrainment, q_t, h, and w can be seen by comparing instantaneous snapshots of the model values of local mass entrainment e, moisture entrainment eq_t, and vertical velocity entrainment ew. Since the Romps (2010) method of calculating e and d requires taking time averages, it is unsuitable for calculating instantaneous entrainment fields. Instead, we use an alternative method that we have devised that substitutes spatial interpolation for time averaging (Dawe and Austin 2011). This alternative method results in slightly smaller values of e and d than those produced by Romps' method, but the two calculations show good agreement in variability. The eq_t and ew fields are calculated simply by multiplying the value of e by the values of q_t and w, respectively.

Comparing the e, eq_t, and ew fields shows that e and eq_t have a very similar spatial pattern, but ew is concentrated in regions where strong updrafts enter the cloud core (Figure 7). The reason for this can been seen by examining the buoyancy, condensed liquid water, and vertical velocity fields that define the cloud core. Of these three fields, buoyancy is the strongest constraint determining if air is part of the core. However, regions exist far above cloud base where air has become negatively buoyant but maintains upward velocity and condensed liquid water. As this air continues to rise more condensation occurs, which heats

the updraft, makes it positively buoyant, and thus entrains it into the core. In this way, entrainment is positively correlated with both q_t and w. This process occurs fairly often in our model cloud field, as evidenced both by our manual examination of the output fields, and the size of the difference between w_{shell} and $w_{entrain}$ in the mean profiles.

6. Discussion

Considering all these results, we now turn to the most important question of all: which entrainment value is the right one? The unsatisfying answer is that it depends on the purpose for which the entrainment is to be used.

Consider a cumulus cloud parametrization based upon a simplified form of the continuity equation which assumes the cloud fraction is constant,

$$\frac{\partial M_{core}}{\partial z} = E - D \tag{14}$$

a cloud budget equation that assumes mean vertical advection is balanced by entrainment of mean environmental properties,

$$M_{core}\frac{\partial \phi_{core}}{\partial z} = E(\phi_{env} - \phi_{core}) \tag{15}$$

and a simple detrainment forcing equation,

$$\rho\frac{\partial \phi_{env}}{\partial t} = D(\phi_{core} - \phi_{env}). \tag{16}$$

ϕ_{env} is input to the parametrization from the GCM. If we assume we have a perfect parametrization of M_{core} and ϕ_{core} at cloud base with which to construct mean core mass flux and tracer profiles, we wish the E and D values to produce a profile of $\partial\phi_{core}/\partial t$ to force the GCM

which agrees with LES results for a similar mean environmental profile. The E and D we desire then is closer to $E_{\phi S}$ and $D_{\phi S}$ than E_d and D_d, but nevertheless must be modified to account for the time tendency and Reynolds flux budget terms we have neglected. This also implies that we should have different $E_{\phi S}$ and $D_{\phi S}$ values for properties with different distribution patterns around the clouds.

Using values near E_d and D_d instead would require modifying equation (15) to

$$M_{core}\frac{\partial \phi_{core}}{\partial z} = E(\phi_{core} - \phi_E) - D(\phi_{core} - \phi_D) \tag{17}$$

and equation (16) into

$$\rho\frac{\partial \phi_{env}}{\partial t} = D(\phi_D - \phi_{env}) - E(\phi_E - \phi_{env}). \tag{18}$$

Now, instead of calculating different E and D values for each tracer we wish to model, we must instead calculate ϕ_E and ϕ_D values for each property that is entrained or detrained. While it is possible this would produce a better parametrization, it seems simpler to fold the effects of ϕ_E and ϕ_D into the E and D values and keep the equations in their less complex form.

On the other hand, the true values of the mass entrainment and detrainment are important for comparison of LES results with field studies, or possibly for calculations of aerosol reactions whose chemical properties are dependent on the concentration of liquid water in the air (Hoppel et al. 1994). They are also vital for diagnosing mass exchanges of individual clouds in an LES ensemble, for which a simple "environment" and "cloud core" mean tracer budget may be difficult to define.

The large positive value of $w_{entrain}$ is clearly inconsistent with the often-made assumption that fluid entrained into the cloud core has negligible vertical momentum (Simpson and

Wiggert 1969; Gregory 2001; Siebesma et al. 2003). This is reflected in the negative magnitude for the transformed E_{wT} shown in Fig. 5b and the smaller value of D_{wT} compared with D_{qT} in Fig. 5c: since w_{env} is slightly negative, the transformed velocity entrainment must be negative to bring positive velocity into the core. The negative w entrainment values (and the large negative detrainment values produced near cloud base for both q_t and w) emphasize the artificial nature of the Siebesma tracer budget entrainment and detrainment. The Siebesma entrainment and detrainment values are mathematical quantities that satisfy both the continuity equation (1) and the tracer budget of the cloud core under the assumption that the core entrains mean environment fluid and detrains mean cloud core fluid.

While the correlations between vertical velocity and entrainment we found were done for cloud core entrainment, we would like to emphasize that this process is not an artifact of the cloud core sampling; similar correlations between entrainment, humidity and vertical velocity appear when we perform entrainment calculations for simple cloudy regions (areas of condensed liquid water). In this case, vertical advection of air can drive condensation, converting environment air into cloud air, and thus driving entrainment of air into the cloud.

As both BOMEX and ARM model runs involved non-precipitating shallow cumulus, we have ignored the effects of precipitation. Precipitation is generally not considered part of the turbulent mixing processes associated with entrainment and detrainment in parametrization, instead being represented by a sink term in the liquid water budget (Tiedtke 1989; Kain and Fritsch 1990). LES bulk microphysics and bin schemes are more complicated, explicitly modeling advection of precipitation by the wind and precipitation fall rate. Nevertheless, incorporating precipitation into the Siebesma tracer budget and direct entrainment calculations would be relatively simple. The precipitation fall rate would be a new sink/source

forcing term in Siebesma's equation (2), and would be part of the forcing term $\rho \mathcal{A} S_\phi$ in Romps' equation (4), resulting in precipitation fall not being counted as part of the detrainment. Specifying the advection terms would be somewhat trickier since, depending on the complexity of the microphysics scheme, moisture might be advected as a single q_t field or advected as separate hydrometeor classes. However, this would simply mean adding extra advection terms for each hydrometeor class. Once these effects were properly incorporated into the calculations, the transformations between (E_d, D_d) and (E_{qT}, D_{qT}) would be unchanged.

7. Conclusion

We have explained the differences between values of entrainment and detrainment of mass calculated via bulk tracer budgets and direct flux calculations by taking into account the properties of the cloud shell, the effect of correlations between local entrainment rates and local air properties, and differences in the numerical methods used by the two calculations. Furthermore, significant correlations are apparent between local tracer values and local entrainment rates. These correlations are the result of upward advection of negatively buoyant, saturated air so that condensation causes latent heating, making the air buoyant and entraining it into the core. These effects suggest that the moist cloud shell has a significant role in mediating fluxes between the clouds and the environment.

Direct entrainment and detrainment calculations should be used to help improve our understanding of the dynamics of cloud mass exchanges and radial variation in cloud properties, with an eye to folding these effects into the simplest cloud parametrization possible.

This should include using the behavior of various tracers to produce different E and D values for q_t and h than for w, and possibly other cloud properties as well. Doing so has the potential to improve GCM parametrization of the magnitude and variability of mass and tracer exchanges between clouds and their environment.

Acknowledgments.

Support for this work was provided by the Canadian Foundation for Climate and Atmospheric Science through the Cloud Aerosol Feedback and Climate network. We thank Marat Khairoutdinov for making SAM available to the cloud modeling community. We would also like to thank David Romps and two anonymous reviewers whose comments significantly improved the quality of this paper. All figures were generated using the matplotlib library in the Python programming language.

APPENDIX

Table of Notation

Table 1 goes here.

REFERENCES

Bechtold, P., M. Koehler, T. Jung, F. Doblas-reyes, M. Leutbecher, M. J. Rodwell, F. Vitart, and G. Balsamo, 2008: Advances in simulating atmospheric variability with the ECMWF model: From synoptic to decadal time-scales. *Q. J. R. Meteorol. Soc.*, **134 (634, Part A)**, 1337–1351, doi:10.1002/qj.289.

Brown, A. R., et al., 2002: Large-eddy simulation of the diurnal cycle of shallow cumulus convection over land. *Q. J. R. Meteorol. Soc.*, **128**, 1075–1093.

Dawe, J. T. and P. H. Austin, 2011: Interpolation of LES cloud surfaces for use in direct calculations of entrainment and detrainment, submitted to Monthly Weather Review.

de Rooy, W. C. and A. P. Siebesma, 2010: Analytical expressions for entrainment and detrainment in cumulus convection. *Q. J. R. Meteorol. Soc.*, **136 (650)**, 1216–1227, doi: 10.1002/qj.640.

Gregory, D., 2001: Estimation of entrainment rate in simple models of convective clouds. *Q. J. R. Meteorol. Soc.*, **127 (571, Part A)**, 53–72.

Heus, T. and H. J. J. Jonker, 2008: Subsiding shells around shallow cumulus clouds. *J. Atmos. Sci.*, **65**, 1003–1018.

Hoppel, W. A., G. M. Frick, J. Fitzgerald, and R. E. Larson, 1994: Marine boundary-layer measurements of new particle formation and the effects nonprecipitating clouds have on aerosol-size distribution. *J. Geophys. Res.-Atmos.*, **99**, 14 443–14 459.

Kain, J. S. and J. M. Fritsch, 1990: A one-dimensional entraining/detraining plume model and its application in convective parameterization. *J. Atmos. Sci.*, **47**, 2784–2802.

Khairoutdinov, M. F. and D. A. Randall, 2003: Cloud resolving modeling of the arm summer 1997 iop: model formulation, results, uncertainties, and sensitivities. *J. Atmos. Sci.*, **60**, 607–625.

Randall, D., et al., 2003: Confronting models with data: The GEWEX cloud systems study. *Bulletin of the American Meteorological Society*, **84 (4)**, 455–469, doi:10.1175/BAMS-84-4-455, URL `http://journals.ametsoc.org/doi/abs/10.1175/BAMS-84-4-455`, `http://journals.ametsoc.org/doi/pdf/10.1175/BAMS-84-4-455`.

Romps, D. M., 2010: A direct measure of entrainment. *J. Atmos. Sci.*, **67 (6)**, 1908–1927.

Rougier, J., D. M. H. Sexton, J. M. Murphy, and D. Stainforth, 2009: Analyzing the climate sensitivity of the HADSM3 climate model using ensembles from different but related experiments. *J. Climate*, **22 (13)**, 3540–3557, doi:10.1175/2008JCLI2533.1.

Siebesma, A. P. and J. W. M. Cuijpers, 1995: Evaluation of parametric assumptions for shallow cumulus convection. *J. Atmos. Sci.*, **52**, 650–666.

Siebesma, A. P., et al., 2003: A large eddy simulation intercomparison study of shallow cumulus convection. *J. Atmos. Sci.*, **60 (10)**, 1201–1219.

Simpson, J. and V. Wiggert, 1969: Models of precipitating cumulus towers. *Mon. Wea. Rev.*, **97 (7)**, 471.

Stainforth, D. A., et al., 2005: Uncertainty in predictions of the climate response to rising levels of greenhouse gases. *Nature*, **433**, 403–406.

Tiedtke, M., 1989: A comprehensive mass flux scheme for cumulus parameterization in large-scale models. *Mon. Wea. Rev.*, **117**, 1779–1800.

Wang, Y. and B. Geerts, 2010: Humidity variations across the edge of trade wind cumuli: Observations and dynamical implications. *Atmos. Res.*, **97 (1-2)**, 144 – 156, doi:DOI:10.1016/j.atmosres.2010.03.017, URL `http://www.sciencedirect.com/science/article/B6V95-4YPPPTH-2/2/7398151adf50038f1b76265010f57c38`.

List of Tables

TABLE 1. List of Symbols

Symbol	Units	Definition	First Occurrence
E, D	kg m^{-3} s^{-1}	Cloud core mass entrainment/detrainment rate	(1)
$E_{\phi S}$, $D_{\phi S}$	kg m^{-3} s^{-1}	Mass entrainment/detrainment rate calculated using Siebesma bulk tracer budget	(2a), (2b)
e, d	kg m^{-3} s^{-1}	Local mass entrainment/detrainment rate	(3)
E_d, D_d	kg m^{-3} s^{-1}	Cloud core mass entrainment/detrainment rate calculated directly from model velocity and tracer fields	§1
$e\phi$, $d\phi$	$[\phi]$ kg m^{-3} s^{-1}	Local cloud core ϕ entrainment/detrainment rate	(4)
$(E\phi)_d$, $(D\phi)_d$	$[\phi]$ kg m^{-3} s^{-1}	Cloud core ϕ entrainment/detrainment rate calculated directly from model velocity and tracer fields	§2
$E_{\phi T}$, $D_{\phi T}$	kg m^{-3} s^{-1}	Cloud core mass entrainment/detrainment rate calculated by transforming a directly calculated value into an equivalent tracer budget value	(9a), (9b)
E_{dT}, D_{dT}	kg m^{-3} s^{-1}	Cloud core mass entrainment/detrainment rate calculated by transforming a tracer budget value into an equivalent directly calculated value	(10a), (10b)
$E_{\phi R}$, $D_{\phi R}$	kg m^{-3} s^{-1}	Cloud core mass entrainment/detrainment rate calculated using Romps bulk tracer budget	(11a), (11b)
ϕ	$[\phi]$	Any fluid tracer, such as q_t (kg kg^{-1}), h (J kg^{-1}), or w (m s^{-1})	§1
ϕ_{core}	$[\phi]$	Mean cloud core ϕ	§3a
ϕ_{edge}	$[\phi]$	Mean cloud edge ϕ	§3a
ϕ_{shell}	$[\phi]$	Mean cloud shell ϕ	§3a
ϕ_{env}	$[\phi]$	Mean environment ϕ	§3a
$\phi_{entrain}$	$[\phi]$	Effective value of ϕ being entrained calculated from direct entrainment	§3b
$\phi_{detrain}$	$[\phi]$	Effective value of ϕ being detrained calculated from direct detrainment	§3b
ϕ_E	$[\phi]$	Placeholder for the value of ϕ assumed to be entraining	(9a)
ϕ_D	$[\phi]$	Placeholder for the value of ϕ assumed to be detraining	(9b)

List of Figures

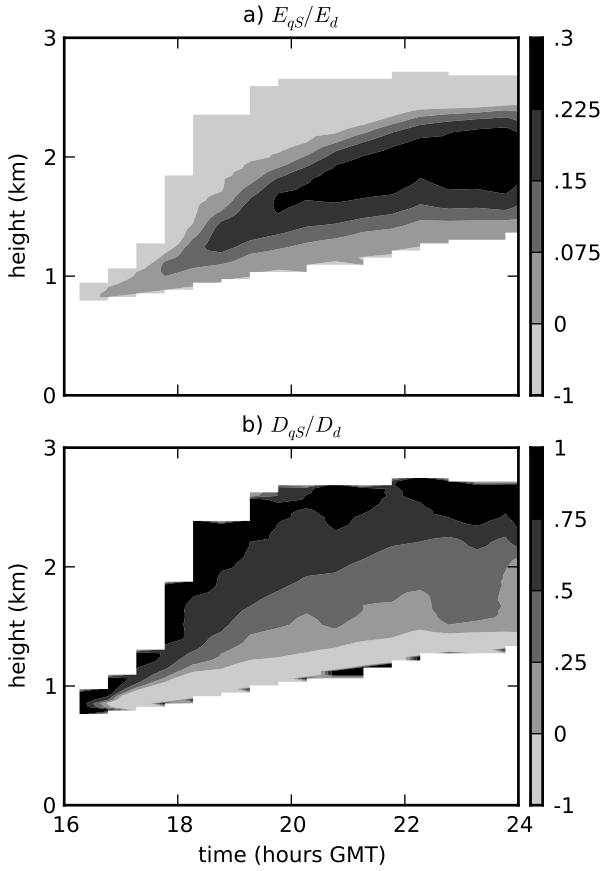

FIG. 1. Variability of the ratio of the Siebesma specific humidity tracer budget a) entrainment and b) detrainment values to the directly calculated values over the duration of the ARM model run.

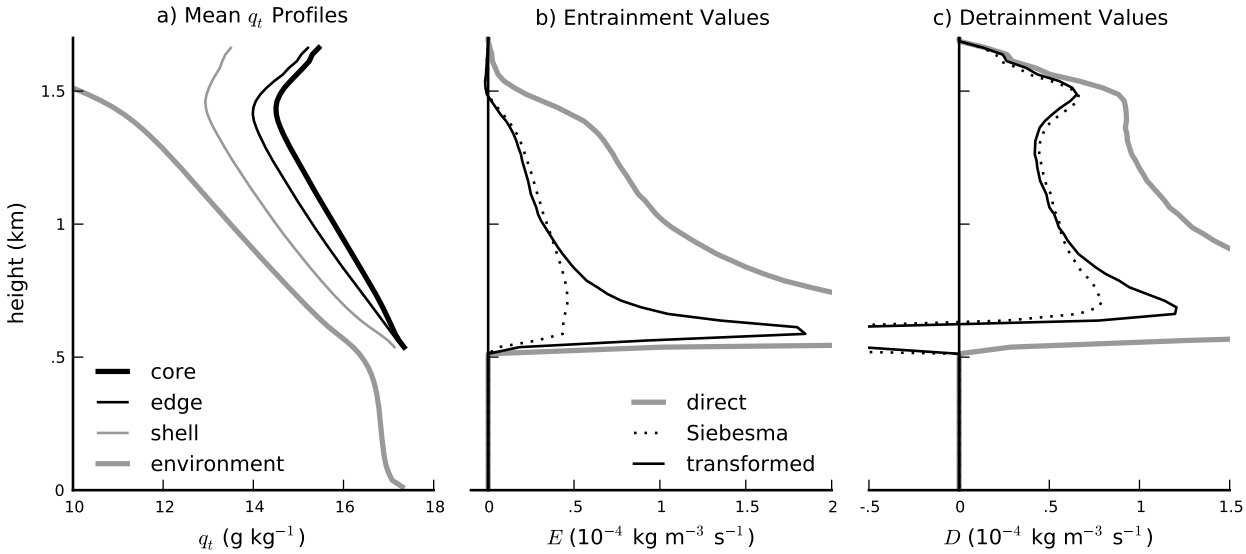

FIG. 2. Result of transforming direct entrainment values into equivalent tracer budget values using mean cloud core shell and edge properties. a) Mean profiles of the total specific humidity in the cloud core (thick black line), cloud core edge (thin black line), cloud core shell (thin grey line), and cloud core environment (thick grey line). These q_t values are used to transform directly calculated values of b) entrainment and c) detrainment (grey line) into equivalent tracer budget values (black line). The Siebesma tracer budget entrainment and detrainment are shown for comparison (dotted lines).

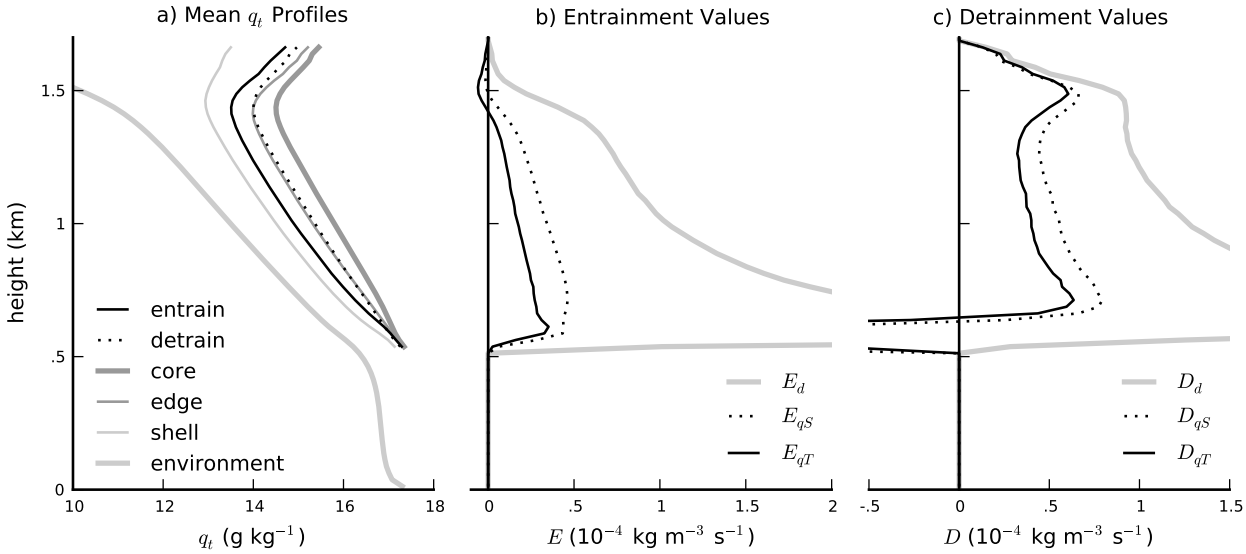

FIG. 3. Result of transforming direct entrainment values into equivalent tracer budget values using effective entrainment and detrainment properties. a) Mean profiles of the effective total specific humidity values being entrained ($q_{entrain}$, black line), and detrained ($q_{detrain}$ dotted line), overlaid on the mean total specific humidity values of the core, edge, shell and environment. These q_t values are used to transform directly calculated values of b) entrainment and c) detrainment (grey line) into equivalent tracer budget values (black line). The Siebesma tracer budget entrainment and detrainment are shown for comparison (dotted lines).

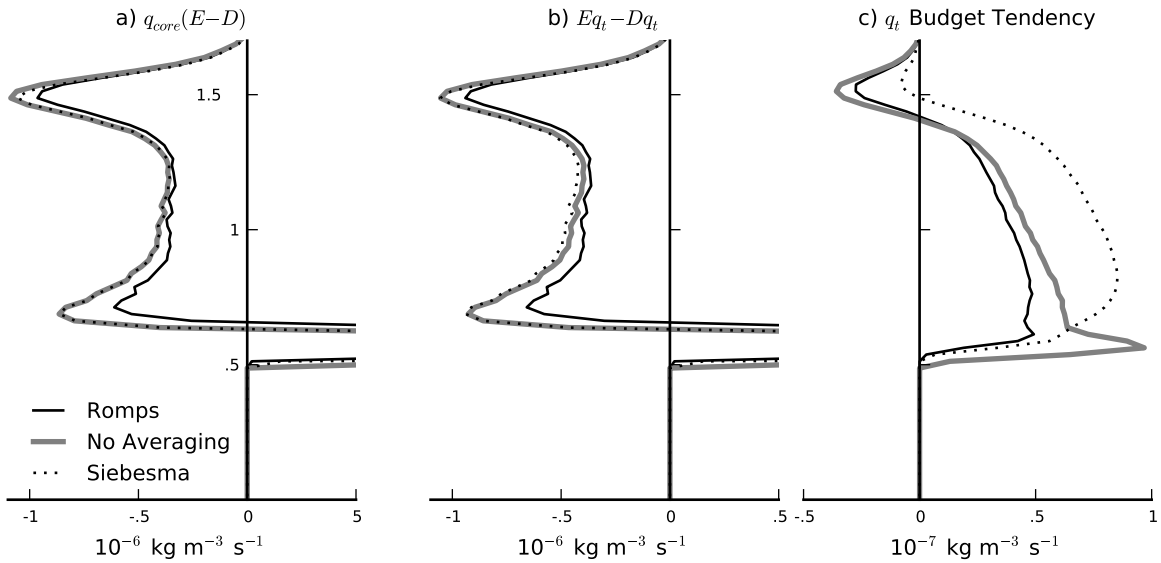

FIG. 4. Size of a) $q_{core}(E-D)$, b) Eq_t-Dq_t and c) the resulting cloud core vertical advection and time tendency specific humidity budget VATT= $q_{core}(E-D)-(Eq_t-Dq_t)$ for the direct entrainment/detrainment (black lines), the direct entrainment/detrainment without time averaging (grey lines), and the Siebesma tracer budget entrainment/detrainment (dotted lines).

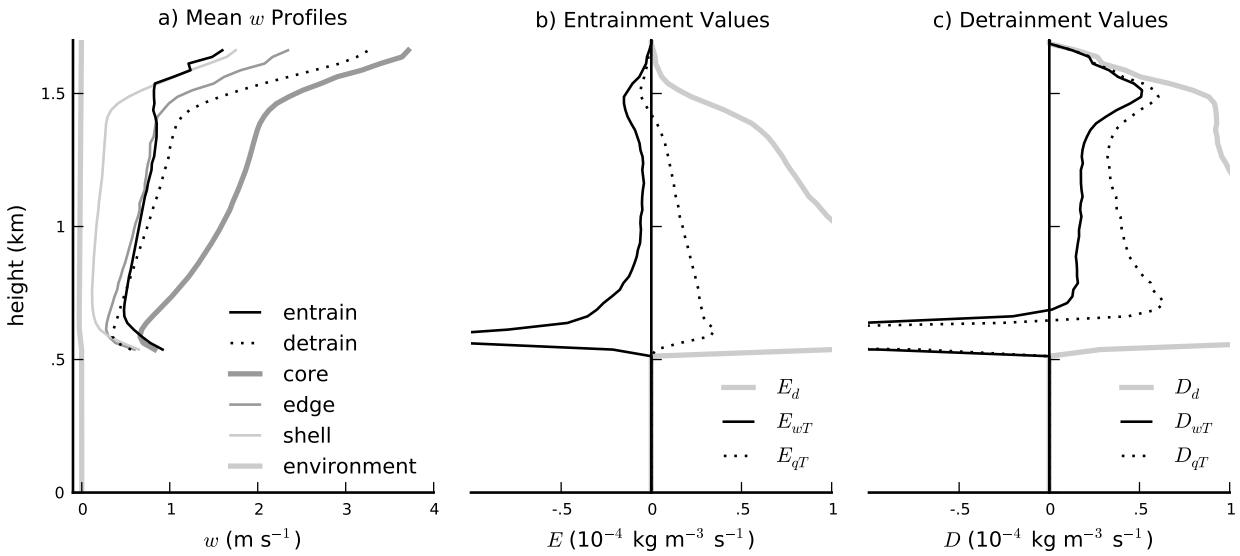

FIG. 5. Result of transforming direct entrainment values into equivalent w budget values. a) Mean profiles of the effective w values being entrained (black line), and detrained (dotted line), overlaid on the mean w values of the core, edge, shell and environment. These w values are used to transform directly calculated values of b) entrainment and c) detrainment (grey line) into equivalent tracer budget values (black line). The entrainment and detrainment values transformed using q_t are shown for comparison (dotted lines).

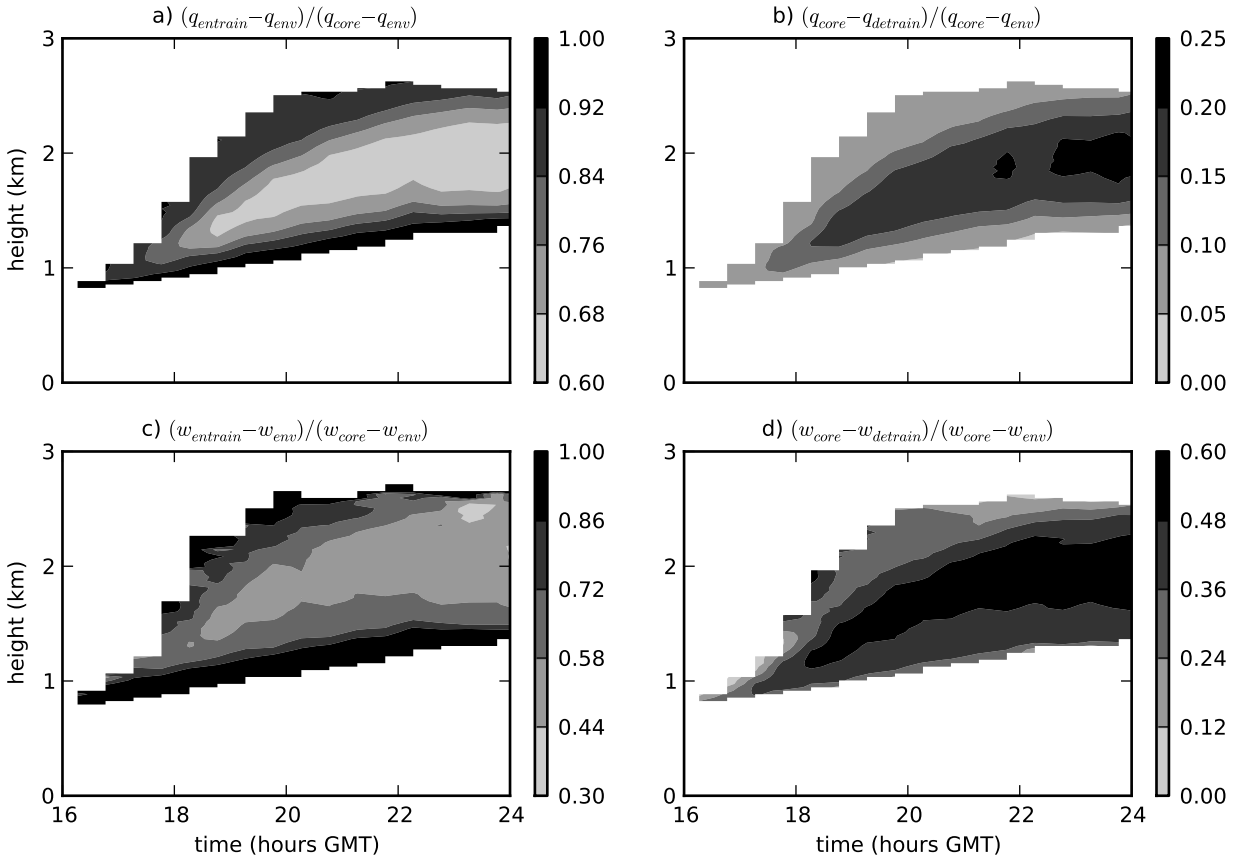

FIG. 6. Variation in a) $(q_{entrain} - q_{env})/(q_{core} - q_{env})$, b) $(q_{core} - q_{detrain})/(q_{core} - q_{env})$, c) $(w_{entrain} - w_{env})/(w_{core} - w_{env})$, and d) $(w_{core} - q_{detrain})/(w_{core} - w_{env})$ over the duration of the ARM model run.

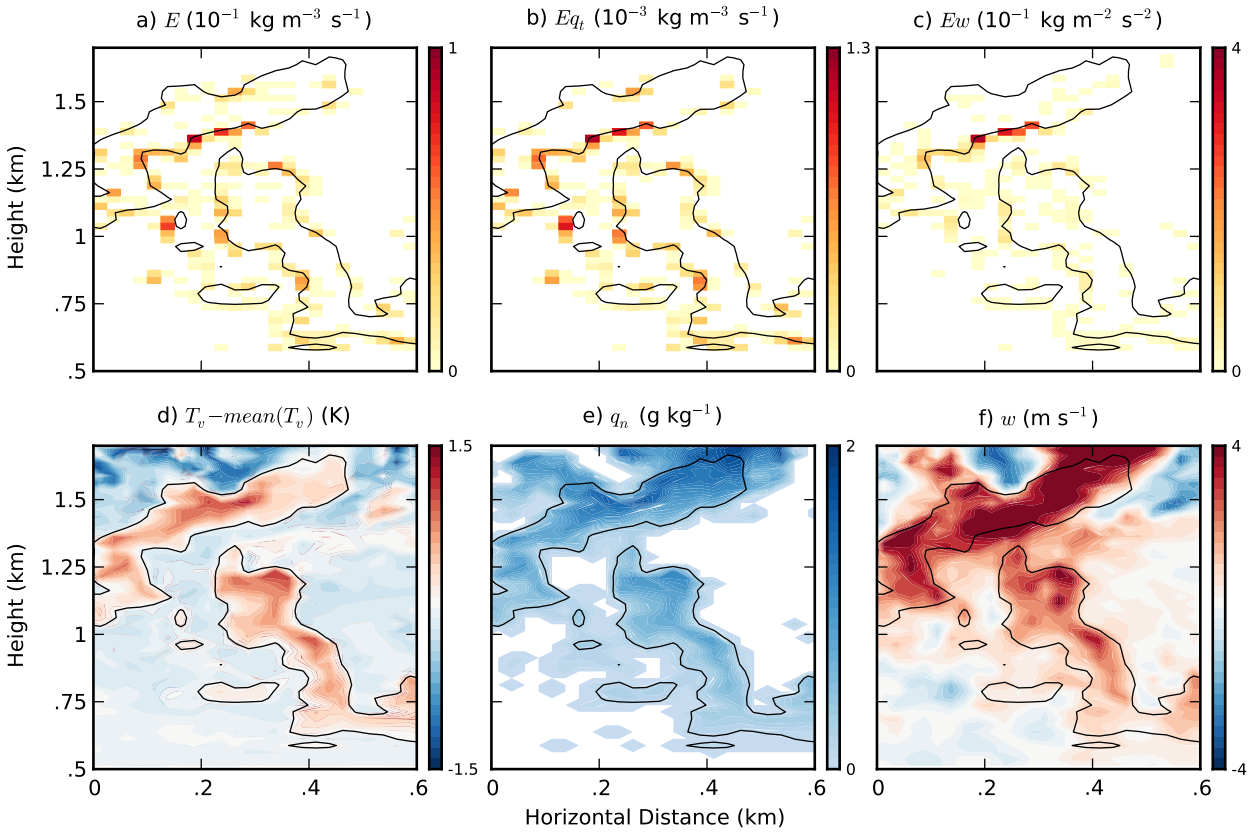

FIG. 7. Instantaneous vertical cross-section of directly calculated cloud core mass entrainment (a), humidity entrainment (b), vertical velocity entrainment (c), buoyancy (d), condensed liquid water (e), and vertical velocity (f) of a single model cloud, illustrating the strong correlation between vertical velocity and entrainment. Black lines indicate the edge of the cloud core in each figure.